ELSEVIER

Contents lists available at ScienceDirect

# Applied Geochemistry

journal homepage: www.elsevier.com/locate/apgeochem



Trace element chemistry and strontium isotope ratios of atmospheric particulate matter reveal air quality impacts from mineral dust, urban pollution, and fireworks in the Wasatch Front, Utah, USA

Micah J. Marcy <sup>a</sup>, Gregory T. Carling <sup>a,\*</sup>, Alyssa N. Thompson <sup>a</sup>, Barry R. Bickmore <sup>a</sup>, Stephen T. Nelson <sup>a</sup>, Kevin A. Rey <sup>a</sup>, Diego P. Fernandez <sup>b</sup>, Matthew Heiner <sup>c</sup>, Bradley R. Adams <sup>d</sup>

- <sup>a</sup> Department of Geological Sciences, Brigham Young University, Provo, UT, USA
- <sup>b</sup> Department of Geology & Geophysics, University of Utah, Salt Lake City, UT, USA
- <sup>c</sup> Department of Statistics, Brigham Young University, Provo, UT, USA
- d Department of Mechanical Engineering, Brigham Young University, Provo, UT, USA

#### ARTICLE INFO

Editorial handling by: JoAnn M Holloway

Keywords:
Dust
Fireworks
Urban pollution
Winter inversions
Strontium isotopes
Trace elements
PCA
Air quality
Particulate matter
Wasatch front

#### ABSTRACT

Atmospheric particulate matter (PM) in urban areas is derived from natural and anthropogenic sources, but it is difficult to identify how these various sources contribute to air quality. To characterize PM sources in an urban setting, we collected PM in three size fractions (PM2.5, PM10, and total suspended particulates, TSP) for two-week intervals from 2019 through 2021 in the Wasatch Front of northern Utah. The PM samples were analyzed for major and trace element concentrations and <sup>87</sup>Sr/<sup>86</sup>Sr ratios. Using principal components analysis, we identified mineral dust, urban pollution, and fireworks as the primary PM sources affecting Wasatch Front air quality. Dust contributed Al, Be, Ca, Fe, Mg, Rb, Y, and REEs, which are typical components of carbonate and silicate minerals, with highest concentrations in the TSP fraction. Urban sources produced PM that was enriched in As, Cd, Mo, Pb, Sb, Se, and Tl, and fireworks smoke had high concentrations of Ba, Cr, Cu, K, Sr, and V. Dust events dominated PM chemistry during spring through fall, punctuated by fireworks smoke over the Independence Day holiday, while urban pollution dominated PM chemistry from November through February during winter inversions. <sup>87</sup>Sr/<sup>86</sup>Sr ratios revealed that Sr was sourced from regional playas, local sediment, and fireworks. Strontium released from fireworks had relatively low <sup>87</sup>Sr/<sup>86</sup>Sr ratios that dominated the PM isotopic composition during holidays. Sequential leaching showed that potentially harmful elements such as Se, Cd, and Cu were readily removed by weak acids, suggesting that they are readily available in the environment or through human inhalation. This is the first study to describe seasonal variations in PM chemistry in the Wasatch Front and serves as an example of investigating air quality in complex urban areas impacted by desert dust.

### 1. Introduction

### 1.1. Background

Air quality in urban areas is affected by atmospheric particulate matter (PM) from natural and anthropogenic sources that are often difficult to disentangle. Increased PM is linked to higher rates of asthma, pneumonia, cardiovascular disease (Pope et al., 1990). Natural PM sources, which are often influenced by human processes, include wild-fire smoke and windblown mineral dust from burned areas and desert regions (Goudie, 2009; Hahnenberger and Nicoll, 2012). Mineral dust

combines with urban PM to create a mixture that is enriched in trace elements (Goodman et al., 2019; Putman et al., 2022; Sudheer and Rengarajan, 2012). Air quality impacts from natural and anthropogenic PM may be exacerbated by local meteorological conditions. For example, wintertime inversions create poor air quality in many western US basins with high pressure-driven persistent cold air pools, which trap local pollution in cold air masses in the valley bottoms (Gillies et al., 2010; Whiteman et al., 2014; Wolyn and McKee, 1989).

Geochemical measurements are used to create "fingerprints", defined by distinct chemical or isotopic characteristics, to identify dust sources from natural or anthropogenic sources. Trace metal chemistry of

<sup>\*</sup> Corresponding author. S389 ESC, Provo, UT, 84602, USA. *E-mail address*: greg.carling@byu.edu (G.T. Carling).

dust varies based on the geologic province, landscape type, or source materials (Aarons et al., 2017). Playa dust contains salts (Abuduwaili et al., 2008) and elevated concentrations of Li, Na, Sr, U, Mg, and Ca in carbonates and other evaporite minerals (Carling et al., 2012; Dastrup et al., 2018; Goodman et al., 2019). Urban PM is often enriched in anthropogenic metals such as Cd, Pb, Zn, and Cu (Sudheer and Rengarajan, 2012), while distinct urban pollution sources may be identified by specific elements. Fireworks smoke contains metals that are used as coloring agents or oxidizers, including Ba, Mg, K, Sr, and Cu (Perry, 1999; Steinhauser et al., 2008; Vecchi et al., 2008). Hourly chemical data in Madrid revealed a close association between traffic flow with metallic emissions (Zn, Cu, Cr, Fe) and resuspended mineral dust (Ca, Al, Si) (Moreno et al., 2013). Emissions from petroleum refineries showed dramatic increases in La and lanthanide concentrations over background conditions (Kulkarni et al., 2007). Fugitive dust from local soils is typically associated with crustal elements like Fe (Sun et al., 2019), while fugitive dust from mining areas may be enriched in heavy metals like Tl, Cu, and Mo (Putman et al., 2022). The bioavailable element metal fraction, or fraction with high reactivity in the environment, may be used as a fingerprint and to determine potential health or environmental impacts from dust (Goodman et al., 2019; Lanno et al., 2004).

Isotopic measurements often provide distinct dust source fingerprints. Strontium isotope (87Sr/86Sr) ratios were used to differentiate dust from source regions across the western US, including alluvium, sand dunes, glacial moraines, and playas (Aarons et al., 2017). Variability in 87Sr/86Sr ratios across western Utah playas provided sufficient leverage for apportioning dust fluxes to downwind urban areas and mountain snowpack (Carling et al., 2020). Isotopic fingerprinting revealed western US dust sources affecting the Uinta Mountains in northern Utah (Munroe et al., 2019). In an urban setting, 87Sr/86Sr ratios were used to demonstrate the importance of local fugitive dust (Putman et al., 2022). A multiple isotope approach (206Pb/204Pb and 87Sr/86Sr) successfully identified urban aerosol sources in Beijing (Widory et al., 2010).

The purpose of our study is to track atmospheric trace element

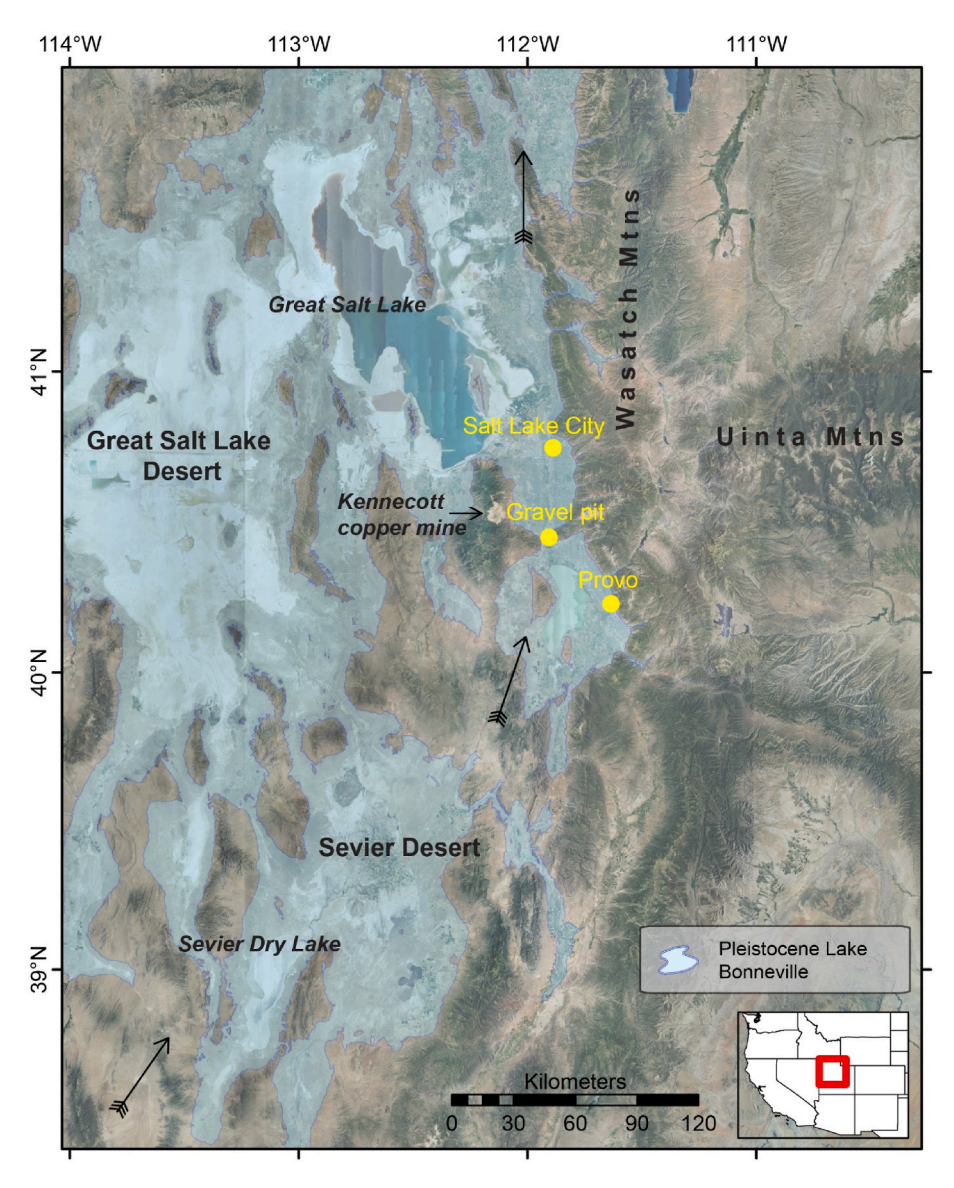


**Fig. 1.** Air particulate matter sampling locations in the Wasatch Front urban area of northern Utah, USA, including Salt Lake City, Provo, and a site downwind of a gravel pit (indicated by yellow dots). Salt Lake City—archived PM<sub>10</sub> filters collected from 2008 to 2009. Provo—PM<sub>2.5</sub>, PM<sub>10</sub>, and TSP filters collected from 2019 to 2021 and marble samples collected during 2021. Gravel pit—PM<sub>10</sub> and TSP filter samples collected during a high wind event in 2021. SrSr/86Sr ratios on our samples were compared with published results on dust from Great Salt Lake, Sevier Dry Lake, and other regional playas. Hatched arrows indicate the prevailing wind direction. Background satellite image taken ca. 2018. Figure modified after Goodman et al. (2019).

chemistry and strontium isotopes in an urban area impacted by mineral dust to evaluate air quality impacts from multiple sources. Specific objectives are to: 1) determine which PM sources have the primary impact on air quality; 2) develop geochemical fingerprints of PM to relate with potential sources; 3) identify specific PM sources using <sup>87</sup>Sr/<sup>86</sup>Sr ratios; and 4) quantify the environmentally available fraction of PM-associated metals. Our study was conducted in the Wasatch Front in northern Utah, an urban area with complex air quality that is impacted by windblown dust events, fugitive dust, winter inversions, and smoke from wildfires and fireworks. Previous studies have shown that local urban and industrial sources contribute to high trace metal concentrations in dust along the Wasatch Front (Goodman et al., 2019; Putman et al., 2022) and that regional dust also impacts downwind snowpack and sensitive alpine areas in the Wasatch and Uinta Mountains (Dastrup et al., 2018; Reynolds et al., 2010, 2014).

### 1.2. Wasatch front study area

The Wasatch Front urban area is home to more than 2.5 million people adjacent to the Wasatch Mountains in northern Utah (Fig. 1). The positioning of the Wasatch Front in a deep basin surrounded by mountains with upwind desert areas creates frequent air quality issues. Windblown dust from dry lakebeds, anthropogenic activities (e.g., construction, mining, oil and gas, grazing, agriculture, fireworks), wildfire smoke, and winter inversions negatively affect air quality at various times of the year.

Dust from upwind desert regions frequently affects Wasatch Front air quality. The Great Salt Lake, Sevier Dry Lake, and other playas across the eastern Great Basin are remnants of Pleistocene Lake Bonneville that act as regional dust "hot spots" (Fig. 1). In November 2022, the Great Salt Lake reached a historic low mark with a  $\sim$ 41% decline in lake surface area relative to 1986-87 (USGS, 2023). Sevier Lake dried due to water diversions in the late 1800s and has remained dry with the exception of high snowmelt years (Oviatt, 1988). Dust is regularly transported from these and other regional playas to urban areas with an average of 4.7 dust events per year since 1930 (Hahnenberger and Nicoll, 2012). Dust events are often associated with strong winds from the southwest during cold fronts or baroclinic troughs during the spring and fall (Hahnenberger and Nicoll, 2012; Nicoll et al., 2020; Steenburgh et al., 2012). Previous work identified distinct <sup>87</sup>Sr/<sup>86</sup>Sr ratios for Sevier Dry Lake ( $\sim$ 0.710) and Great Salt Lake ( $\sim$ 0.715) that are useful for tracking dust from playa sources (Carling et al., 2020). Fugitive dust from industrial activities also impacts the Wasatch Front, including dust from many active and legacy gravel pits, roads, construction, and the Kennecott open pit copper mine and associated refining and smelting operations (Putman et al., 2022).

The Wasatch Front is affected by winter inversions that typically occur during December through February. Several studies have examined the mechanisms of Wasatch Front air pollution during persistent cold air pools (Gillies et al., 2010; Whiteman et al., 2014; Wolyn and McKee, 1989) but none have examined atmospheric trace element chemistry during inversions.

Fireworks are used in holidays and festivals along the Wasatch Front. Though fireworks are usually illegal because of the high fire risk, they are permitted around Independence Day (4 July), Pioneer Day (24 July), and New Year's Eve (31 December). The Utah Department of Air Quality monitors  $\rm PM_{2.5}$  and  $\rm PM_{10}$  concentrations year-round but no studies have directly measured atmospheric metal concentrations during fireworks events along the Wasatch Front.

### 2. Methods

## 2.1. Active air particulate matter sampling

To evaluate the major and trace element chemistry of Wasatch Front PM, we installed three AirMetrics MiniVol TAS Portable Air Samplers with filters collecting  $PM_{2.5}$ ,  $PM_{10}$  and total suspended particulate (TSP) fractions at Brigham Young University in Provo (Fig. 1).  $PM_{2.5}$  and  $PM_{10}$  are fine particles with an aerodynamic diameter less than 2.5 and  $10~\mu m$ , respectively. The samplers operated at a flow rate of 5 L/min with Teflon filters. Collectors were placed on the roof top of a four-story building to minimize PM inputs from local sources. Filters were replaced every two weeks for continuous collection of TSP (n=56) from June 2019 through August 2021 and  $PM_{2.5}$  (n=52) and  $PM_{10}$  (n=50) from July 2019 through July 2021. The number of samples is different for each size fraction because some samples were lost due to equipment malfunction or errors with processing filters. The resulting "Provo filter" dataset provides a nearly continuous two-year record of size-fractionated PM chemistry at Provo with 14-day integrated samples.

To compare with samples collected at Provo and to expand the geographic area of our study, we obtained archived  $PM_{10}$  filters (n=29) from the Utah Division of Air Quality to develop a small "Salt Lake City filter" dataset. The filters were collected at Hawthorne Elementary School in Salt Lake City (Fig. 1) between August 2008 and September 2009. The samplers collected  $PM_{10}$  for 24-h periods at a flow rate of 16.7 L/min with Teflon filters.

#### 2.2. Bulk deposition sampling

To characterize potential differences between active air filter samples and passive bulk samples that collect both wet and dry deposition, a separate marble collector was placed adjacent to the MiniVol air samplers at our Provo site (Fig. 1). Bulk deposition was collected in a 190 L tote that was lined with a plastic bag and covered with an acid-leached plastic screen and marbles to provide a surface for dust deposition (Goodman et al., 2019; Reheis and Kihl, 1995). Samples were collected from February 2021 to September 2021 with six-week deployment periods, providing five bulk atmospheric deposition samples in a "Provo marble" dataset. The longer deployment for passive bulk deposition (six weeks) compared with active air filters (two weeks) was necessary to collect sufficient material for geochemical analysis. At the end of each sampling period, the marbles and screen were rinsed with Milli-Q water before the plastic bag was removed from the tote. The resulting slurry was then transferred into acid-rinsed 2 L FLPE bottles. Sample slurries were evaporated at 60  $^{\circ}$ C until  $\sim$ 5 mL remained and then left to dry at room temperature.

### 2.3. Dust source sampling

To characterize the local dust signature along the Wasatch Front from a specific point source, we placed two MiniVol air samplers downwind of a gravel pit midway between Provo and Salt Lake City (Fig. 1) during a high-wind event on 19 September 2021 to collect TSP and  $PM_{10}$  fugitive dust samples. Gravel at the pit is derived from Lake Bonneville sediments and crushed local bedrock. Air samplers were placed at other gravel pit locations but there was insufficient material collected for analyses.

# 2.4. Geochemical analysis of filters and bulk deposition samples

All Provo filter (n=158), Salt Lake City filter (n=29), gravel pit filter (n=2), and Provo marble bulk deposition (n=5) samples were analyzed for major and trace element concentrations following a sequential leaching process. Filter samples were prepared for analysis following a two-step sequential acid leaching procedure selected to quantify the readily leachable or environmentally available fraction (acetic acid) and the residual fraction (aqua regia). The total element concentration was calculated as the sum of both leaching steps. Filters were folded to fit inside an acid-washed 50 mL centrifuge tube. We added 7 mL of 1 M acetic acid (CH<sub>3</sub>COOH) to each tube and placed the samples on a shaker table for  $\sim$ 24 h. Samples were centrifuged at 4000 rpm for 3–6 min and decanted by pipetting into acid-washed 15 mL

centrifuge tubes. The leaching process was then repeated with 6 mL of aqua regia (1:3 ratio of concentrated nitric acid to hydrochloric acid).

The Provo marble samples were subjected to a four-step sequential leaching procedure, given a larger sample mass compared with filter samples. We used 4 mL of 1 M ammonium acetate (NH<sub>4</sub>AcO) adjusted to pH = 7, 1 M acetic acid (CH<sub>3</sub>COOH), 1 M nitric acid (HNO<sub>3</sub>), and aqua regia to identify element concentrations from different mineral fractions in the bulk deposition samples. Ammonium acetate extracts the water-soluble and exchangeable fractions, acetic acid extracts the carbonate mineral fraction, nitric acid extracts the clay and feldspar fraction, and aqua regia extracts the residual fraction, though not all remaining material was completely dissolved (Goodman et al., 2019; Naiman et al., 2000; Whiteman et al., 2014).

Sample leachates were analyzed for major and trace element concentrations using an Agilent 7500 cc quadrupole inductively coupled plasma mass spectrometer (ICP-MS) with a collision cell, a double-pass spray chamber with a perfluoroalkoxy nebulizer (0.1 mL/min), a quartz torch, and platinum cones. The samples were analyzed for concentrations of 44 elements including Ag, Al, As, B, Ba, Be, Ca, Cd, Ce, Co, Cr, Cs, Cu, Dy, Er, Eu, Fe, Gd, Ho, K, La, Li, Lu, Mg, Mn, Mo, Na, Nd, Ni, Pb, Pr, Rb, Sb, Se, Sm, Sr, Tb, Th, Tl, U, V, Y, Yb, and Zn.

Samples with sufficient Sr concentration in the acetic acid fraction (>40 ppb Sr; n=164) were analyzed for <sup>87</sup>Sr/<sup>86</sup>Sr ratios using a Thermo-Fisher Scientific Neptune Plus multicollector ICP-MS. The acetic acid effectively reacts with the carbonate mineral fraction to remove Sr for <sup>87</sup>Sr/<sup>86</sup>Sr analysis (Carling et al., 2020). The samples were purified inline using a Sr-FAST ion chromatographic column packed with crown ether resin (Mackey and Fernandez, 2011). Analytical precision (2 $\sigma$ SE) ranged from  $\pm 8 \times 10^{-5} - 8 \times 10^{-6}$ . The <sup>87</sup>Sr/<sup>86</sup>Sr ratios were corrected for mass bias using exponential law, normalizing to <sup>87</sup>Sr/<sup>86</sup>Sr = 0.1194 (Steiger and Jäger, 1977). Isobaric interferences, such as from <sup>87</sup>Rb and <sup>86</sup>Kr, were corrected simultaneously monitoring <sup>85</sup>Rb and <sup>83</sup>Kr using the corresponding invariant ratios of <sup>87</sup>Rb/<sup>85</sup>Rb = 0.385706 and <sup>86</sup>Kr/<sup>83</sup>Kr = 1.502522 (Steiger and Jäger, 1977).

## 2.5. Time-series plots and principal components analysis

A variety of methods are used to identify PM sources including principal components analysis (PCA). PCA is an exploratory technique that is used to reduce multiple variables in an analytical dataset into a small number of factors or principal components (PCs). The PCs may be interpreted as distinct sources, making the technique useful for narrowing down the number of sources affecting air quality (Goodman et al., 2019; Miller-Schulze et al., 2015; Putman et al., 2022).

To create time-series plots and to run a PCA for the Provo filter dataset, we used total element concentrations (i.e., concentrations summed from the acetic acid and aqua regia leachates) expressed relative to volume of air passing through the filter. The volumetric or atmospheric concentrations were expressed as element mass (ng) per volume (m<sup>3</sup>). The PCA was performed in MATLAB using z-scored data for  $PM_{2.5}$ ,  $PM_{10}$ , and TSP filters (n = 152). Standardized (z-scored) data was necessary for the PCA because concentrations varied widely across elements. The PCA scores for PC1, PC2, and PC3 were also plotted as a time series to investigate seasonal changes in air chemistry. Prior to running the PCA, some elements or samples were removed or adjusted for different reasons. The element Ag was below DL in nearly all samples and was removed from the dataset. For other elements with only a few nondetect values, concentrations < DL in specific samples were arbitrarily set to 1/2 the minimum measured element concentration in the dataset. Data from six  $PM_{2.5}$  filters containing <0.1 mg sample mass were removed from further analysis because the low sample mass resulted in inaccurate element concentrations.

#### 3. Results

# 3.1. Concentration time series show air quality impacts from fireworks and urban pollution

We analyzed the trace and major element chemistry from our Provo filter dataset, with two-years of PM<sub>2.5</sub>, PM<sub>10</sub>, and TSP data, for temporal trends in the raw data. Two sources, fireworks and winter urban pollution, were identified from the time-series plots by their clear episodic patterns. The fireworks-related elements Ba, Cu, K, and Sr had the highest concentrations around the Independence Day holiday in 2019, 2020, and 2021 (Fig. 2). Concentrations of these elements increased three to sevenfold during July 2019 and July 2020 relative to the preceding months, with smaller peaks during July 2021. The fireworks elements were elevated in the PM2.5, PM10, and TSP samples across multiple sampling periods, although not always elevated in all size fractions during all years possibly due to variable winds or fireworks emissions year-to-year. During July 2019, the highest concentrations of all four elements were found in the  $PM_{2.5}$  fraction, whereas concentrations were highest in the PM<sub>10</sub> and TSP fractions during July 2020. New Year's Eve fireworks were not readily identifiable in raw chemistry data, but there were small peaks in Ba, Cu, and Sr concentrations during January 2020 and January 2021. The January peaks may be related to fireworks or other sources such as urban pollution.

The urban pollution-related elements As, Cd, Pb, and Tl showed the highest concentrations during winter months (Fig. 3). Concentrations were highest in the TSP fraction and lowest in the PM<sub>2.5</sub> fraction. The increase over background concentrations typically occurred during winter months from mid-November through mid-February, when winter inversions commonly result in elevated atmospheric PM concentrations. Concentrations of As, Cd, Pb, and Tl were higher during winter 2020-21 relative to 2019–20. During winter 2020–21, these elements had two to fourfold higher concentrations than the average summer values. Although Pb concentrations were relatively high during winter, they did not exceed the National Ambient Air Quality Standard (NAAQS) of 0.15  $\mu g/m^3$  over a rolling 3-month average (https://www.epa.gov/criteria-air-pollutants/naaqs-table#1). Maximum Pb concentrations measured in TSP at Provo were at 0.02  $\mu g/m^3$  during January 2021, well below the NAAQS standard.

Other factors influencing air quality were not readily identifiable from the raw time-series data. For example, episodic dust events were not observed in the raw data as expected. Elements associated with mineral dust (e.g., Al, Ca, Fe, Mg, and REEs) were highest in TSP and lowest in PM $_{2.5}$  throughout the study period, but spikes in these elements were not observed. The lack of spikes in dust-associated element concentrations is likely due to the relatively long sampling frequency (filters collected every two weeks) compared with the short duration of dust events, which typically last for several hours up to one day.

# 3.2. Principal components analysis reveals distinct PM sources including mineral dust, fireworks, and urban pollution

The PCA results for the Provo filter dataset revealed additional air quality information that was not readily observable in the raw concentration time-series data, permitting the identification of elements associated with mineral dust. The PCA, using total trace and major element concentrations from  $PM_{2.5}$ ,  $PM_{10}$ , and TSP filters, revealed three principal components (PCs) that explained 82.2% of the variance in the dataset (Fig. 4). The remaining PCs described only a small amount of variability and were not considered further. PC1 retained 63.4% of the variance and is most explained by Al, Be, Ca, Fe, Mg, Rb, Y, and REEs. PC2 retained 10.9% of the variance and is most explained by As, Cd, Mo, Pb, Sb, Se, and Tl. PC3 retained 7.9% of the variance and is most explained by Ba, Cr, Cu, K, Sr, and V. The principal component coefficients showing element contributions to PC1, PC2, and PC3 are shown in the Supplementary material (Fig. S1).

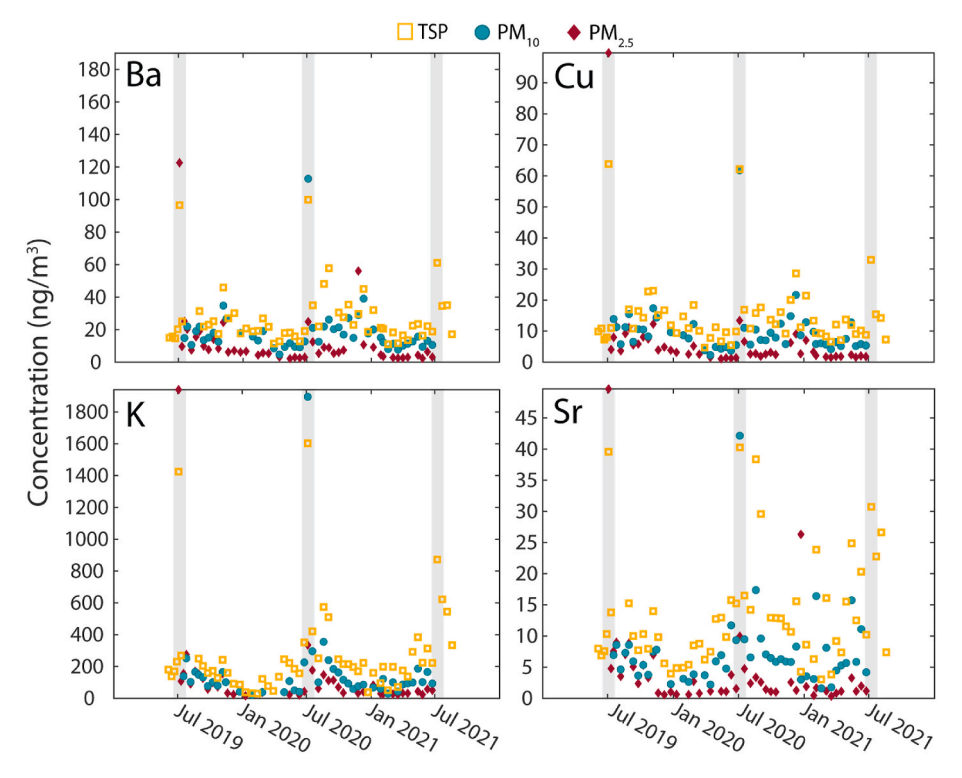


Fig. 2. Total concentrations of elements typically found in fireworks. Spikes in element concentrations occurred around the Independence Day holiday in July (indicated with gray bars) each year. Smaller peaks occurred in element concentrations during other times due to fireworks or other sources.

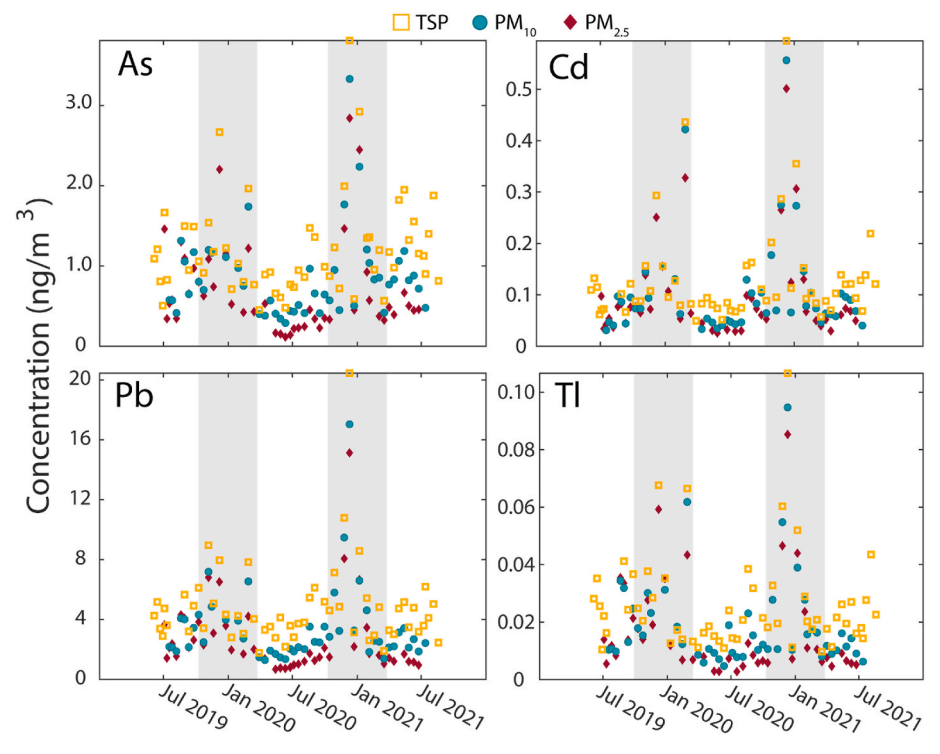


Fig. 3. Total concentrations of elements that were elevated during winter months. Gray bars indicate the winter season (mid-November to mid-February) when inversions typically occur along the Wasatch Front.

The samples were generally separated by PM size along PC1, with  $PM_{2.5}$  samples plotting on the negative end and TSP samples on the positive end of PC1, and  $PM_{10}$  samples in the middle. Spread along PC2 was independent of PM size, with a similar range among the different size fractions. Samples from the Independence Day holiday (4 July 2019

and 2020) plotted separately from the other samples in the plot of PC2 versus PC3, including one  $PM_{2.5}$ , one  $PM_{10}$ , and two TSP samples on the positive end of PC3.

We interpret the three PCs to represent mineral dust, urban pollution, and fireworks smoke. PC1 includes elements commonly found in

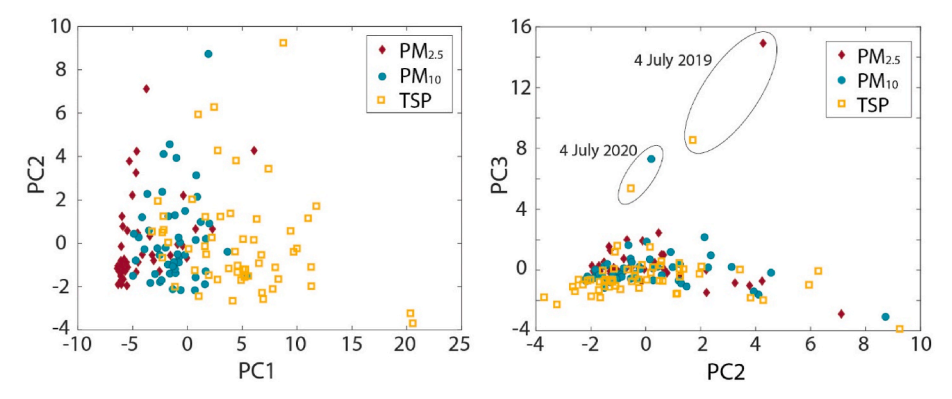


Fig. 4. PCA results on all filter samples collected at Provo. PC1 explains 63.4% of the variance in the data and is most associated with the elements Al, Be, Ca, Fe, Mg, Rb, Y, and REEs. These elements are commonly found in carbonate and silicate minerals in dust. PC2 explains 10.9% of the variance and is most associated with the elements As, Cd, Mo, Pb, Sb, and Tl. These elements are commonly found in anthropogenic pollution that is concentrated during winter months. PC3 explains 7.9% of the variance and is most associated with the elements Ba, Cr, Cu, K, Sr, and V. These elements are commonly found in fireworks.

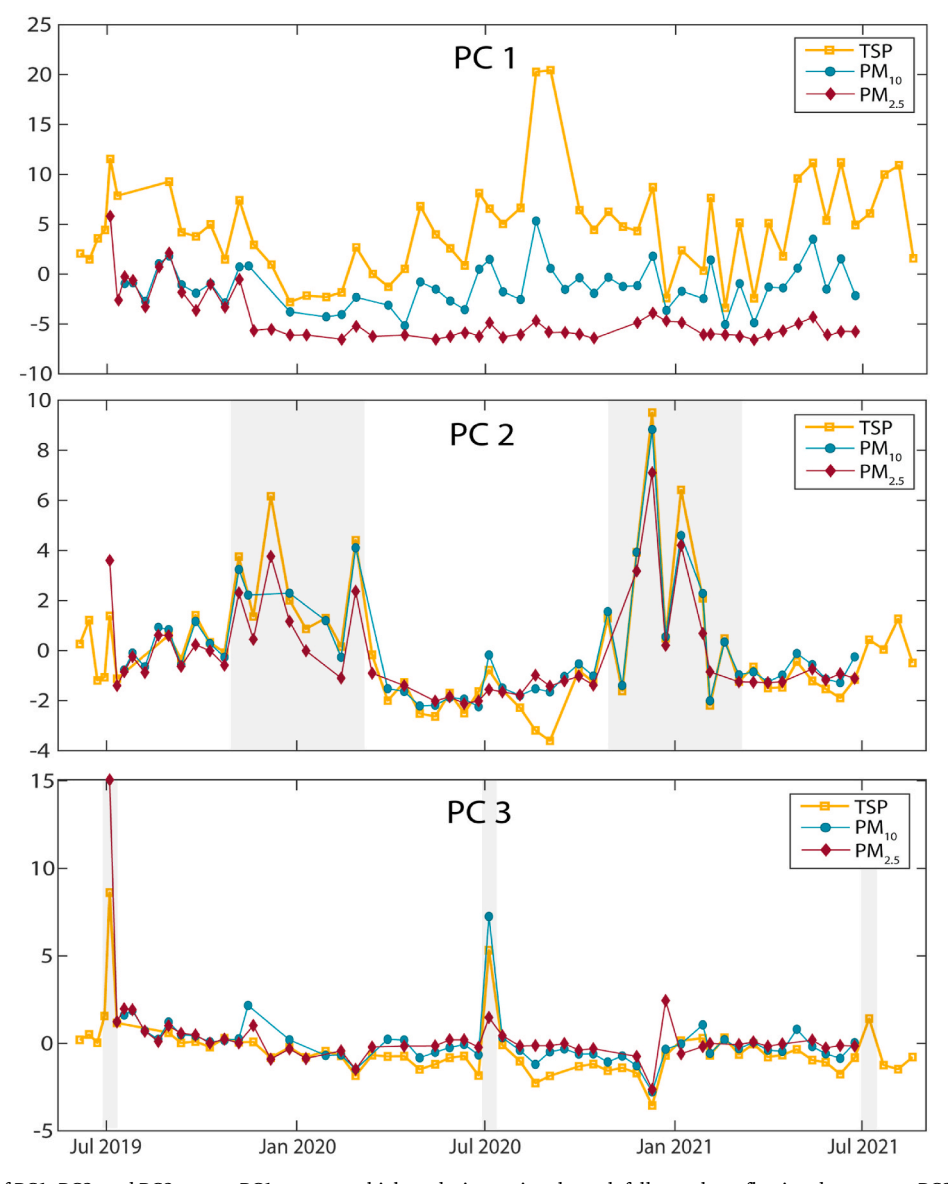


Fig. 5. Time-series plots of PC1, PC2, and PC3 scores. PC1 scores are highest during spring through fall samples reflecting dust events. PC2 scores are highest during winter months reflecting urban pollution during winter inversions. PC3 scores show spikes during the Independence Day holiday in July of 2019 and 2020.

silicate and carbonate minerals. Elements related to mineral dust had the greatest variation in concentrations in the TSP samples, while  $PM_{2.5}$  samples showed little variation over the study period. The average PM size of dust transported to the Wasatch Front is 15–31  $\mu m$  (Goodman et al., 2019), which is best represented by the TSP samples. We assume that only a small amount of mineral dust is captured on the  $PM_{2.5}$  or  $PM_{10}$  filters relative to the TSP filters. PC2 includes elements commonly found in winter pollution during inversions, overlapping with the observation of elevated As, Cd, Pb, and Tl from the raw time-series data (Fig. 3). PC3 includes elements commonly found in fireworks smoke, overlapping with the raw time-series data showing elevated Ba, Cu, K, and Sr concentrations during July (Fig. 2).

The three PCs show distinct patterns when plotted as a time series of PC scores (Fig. 5), providing further evidence for air quality impacts from mineral dust, winter urban pollution, and fireworks smoke. The PC1 time series shows elevated scores during spring through fall and low scores during winter, reflecting seasonal dust events affecting the Wasatch Front. Dust storms typically impact the Wasatch Front during spring through fall when dust sources are dry and emissive and strong storm tracks carry dust from regional playas to the urban area (Steenburgh et al., 2012). The TSP fractions had the highest PC1 scores and  $PM_{2.5}$  had the lowest scores due to the larger particle size of mineral dust

The PC2 time series shows relatively high scores during winter and low scores during summer, highlighting the impacts of winter inversions on the concentrations of PC2-related elements (Fig. 5). The PC3 scores spiked during July 2019 and July 2020, with moderate spikes during January 2021 and July 2021 (Fig. 5). The PC time-series plots confirm observations of fireworks-related elements (Fig. 2) and urban pollution-related elements (Fig. 3) in the concentration time-series plots.

# 3.3. Dust events, fireworks, and local PM sources impact urban Sr isotope ratios

Strontium provides an interesting example for identifying dust sources because it may come from both natural and anthropogenic processes. Notably, Sr showed a mixed signal in the concentration time-series data (Fig. 2) and was grouped with fireworks smoke in the PCA (Fig. 4). We used Sr isotope (<sup>87</sup>Sr/<sup>86</sup>Sr) ratios in the Provo and Salt Lake City filter datasets to evaluate changing Sr inputs to the Wasatch Front over time. Further, we compared <sup>87</sup>Sr/<sup>86</sup>Sr ratios in the Provo filter and marble datasets to evaluate potential differences in sampling methods. The <sup>87</sup>Sr/<sup>86</sup>Sr ratios of our samples were compared with <sup>87</sup>Sr/<sup>86</sup>Sr values of potential sources from the literature and from our new gravel pit samples.

Strontium isotope (87Sr/86Sr) ratios on the Provo filters ranged widely from 0.70796 to 0.71212 during the sampling period of June 2019 through August 2021, with relatively higher ratios in Salt Lake City filters ranging from 0.70945 to 0.71538 from August 2008 through September 2009 (Fig. 6). Annual minima for Provo and Salt Lake City occurred around Independence Day at both sites across multiple years. <sup>87</sup>Sr/<sup>86</sup>Sr ratios in Provo showed moderate seasonal variations, with the highest ratios during summer months (other than the low values on Independence Day). For comparison with a potential dust source, <sup>87</sup>Sr/<sup>86</sup>Sr ratios from gravel pit dust in the Wasatch Front were 0.71236 and 0.71228 on PM<sub>10</sub> and TSP filters, respectively.

The  $^{87}$ Sr/ $^{86}$ Sr ratios were consistent across size fractions and sampling methods. In the Provo filter samples,  $^{87}$ Sr/ $^{86}$ Sr ratios were similar across size fractions for most sets of corresponding TSP and PM<sub>10</sub> filters. The  $^{87}$ Sr/ $^{86}$ Sr ratios of bulk deposition marble samples showed small differences relative to corresponding TSP filters when both sample types were collected over six-week periods at Provo, with differences ranging

**Table 1**Comparison of <sup>87</sup>Sr/<sup>86</sup>Sr ratios in bulk deposition from marble samplers and TSP filters at Provo.

Date Range	Bulk marble (6 weeks)	TSP (6-week average)	Difference
2/26/21-4/8/21	0.71045	0.71056	-0.00011
4/8/21-5/20/21	0.71055	0.71115	-0.00060
5/20/21-7/1/21	0.71044	0.71035	0.00009
7/1/21-8/12/21	0.70929	0.70914	0.00015

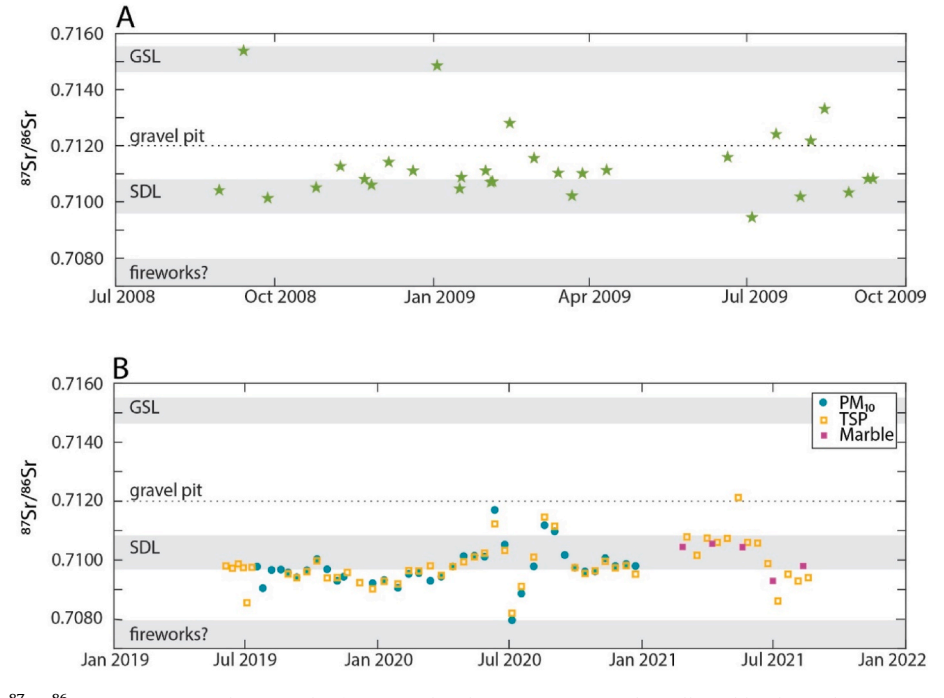


Fig. 6. Strontium isotope ( $^{87}$ Sr/ $^{86}$ Sr) ratios measured on samples from A) Salt Lake City (PM<sub>10</sub> samples collected by the Utah Division of Air Quality) and B) Provo (PM<sub>10</sub>, TSP, and bulk marble samples). Values for Great Salt Lake (GSL) and Sevier Dry Lake (SDL) are from Carling et al. (2020). The dashed line for "gravel pit" is the average  $^{87}$ Sr/ $^{86}$ Sr ratios of two samples collected downwind of gravel mining operations targeting Lake Bonneville shoreline sediments and crushed bedrock. The gray box for "fireworks?" represents an estimated value for the  $^{87}$ Sr/ $^{86}$ Sr ratio of fireworks smoke.

from  $9\times10^{-5}$  to  $6\times10^{-4}$  (Table 1). Compared with  $^{87}\text{Sr}/^{86}\text{Sr}$  measurement errors of  $\pm8\times10^{-5}$ –  $8\times10^{-6}$ , the differences were significant for these samples collected using different methods and may reflect contributions from wet deposition to the bulk marble samples. One TSP sample collected in May 2021 was much higher than the corresponding marble sample for that period (Fig. 6). However, from a practical standpoint, both methods (bulk marbles and TSP filters) provided comparable results for most samples sets collected over the same period. The advantage of active samplers is that the increased sampling rate allows for shorter time-integrated samples to show  $^{87}\text{Sr}/^{86}\text{Sr}$  ratios for specific events (e.g., fireworks or dust events). The differences in specific sample sets may be related to short-lived events that are captured by the filters but "diluted" in the bulk samples.

# 3.4. Sequential leaching results show variability in element removal by weak acids

The environmentally available fraction of trace and major elements in urban PM from the Provo filter and Provo marble samples was evaluated through a sequential leaching process, showing variability in element removal with a weak acid leach (Fig. 7). For the Provo filter dataset, we focused on the TSP filters for simplicity because the different size fractions (PM2.5, PM10, and TSP) showed similar trends. The TSP filters (n = 56) and bulk marble samples (n = 5) were averaged in their respective groups to show general trends and sorted by the percentage of element mass removed with ammonium acetate plus acetic acid in the bulk marble samples. On the TSP filters, Ca, Cd, Mg, Na, Sr, and Zn were readily leached by acetic acid, accounting for over 70% of element mass. Notable toxic elements with >50% abundance removed with the acetic acid leachate included As, Ba, Be, Cd, Co, Cu, La, Mo, Pb, Se, U and Tl. In the bulk marble samples, over half of the As, Ba, B, Ca, Cd, Cu, K, Mg, Mo, Mn, Na, Se, Sr, U, and Zn mass was removed with the ammonium acetate and acetic acid fractions.

#### 4. Discussion

# 4.1. Sources of trace and major elements contributing to air pollution along the Wasatch front

We identified mineral dust, urban pollution, and fireworks smoke as the primary sources of atmospheric trace and major elements to the Wasatch Front. Other sources certainly contribute to air pollution and airborne PM, but these three sources were clearly identified from timeseries plots of raw element concentrations and principal component scores. Within these three categories, fireworks smoke is a distinct source whereas mineral dust and urban pollution are generated from a variety of sources. Our dataset does not allow us to pinpoint the exact sources of mineral dust or urban pollution affecting Wasatch Front air quality, but we are able to generalize trace element sources based on our observations combined with the published literature.

One limitation of identifying sources in a complex urban environment is that specific trace elements may come from multiple sources, as described for Sr in section 3.3. Each element in the dataset contributes to all the PCs, but some elements are *most* associated with specific PCs. For example, Cu and Ba contribute a small amount to PC1 and PC2 but they mostly contribute to PC3 (Supplementary material, Fig. S1). In other words, Cu are Ba are found in mineral dust and urban pollution but are most associated with fireworks smoke in our dataset. Both Cu and Ba show minor peaks during winter reflecting contributions from urban pollution, but the largest peaks occur during July from fireworks (Fig. 2). The subset of elements that most describe a PC can be linked to a specific source based on knowledge of the element groupings, but it is not always possible to directly correlate a PC to a specific source (Goodman et al., 2019; Putman et al., 2022). Further, the three PCs explained a substantial amount of variability in the dataset (combined 82.2%) but not all the variability, suggesting that other sources also impact air quality. Because of these limitations we do not use PCA for source apportionment. Rather, we use PCA to look at trends in the

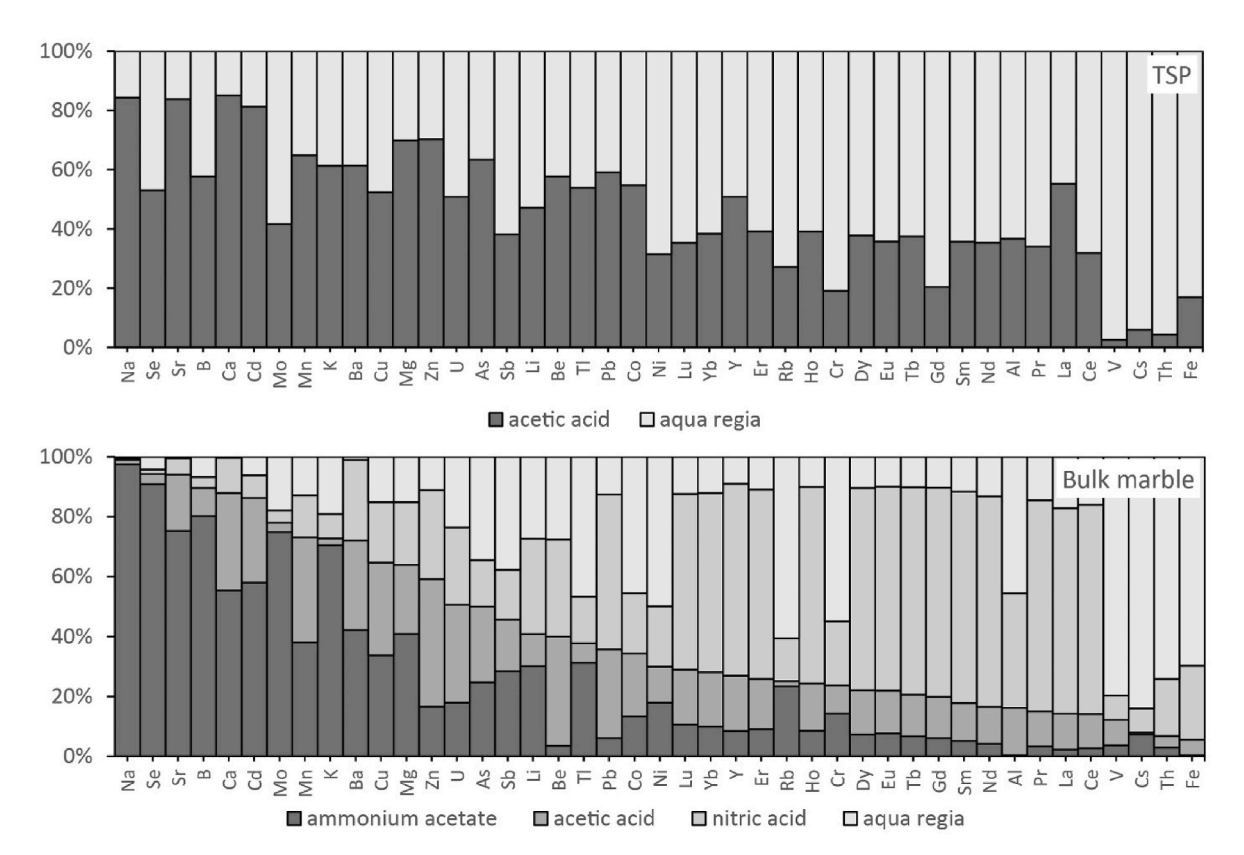


Fig. 7. Fraction of element concentrations in each leachate for TSP filters (n = 56; above) and bulk marble samples (n = 5; below) collected at Provo.

geochemical data and to describe potential element sources based on groupings with other elements. A positive matrix factorization would be useful for source apportionment if the source profiles were more adequately characterized (Hopke et al., 2020).

Mineral dust represents background PM pollution to the Wasatch front, with PM sources including dust emissions from regional playas and fugitive dust from local sources such as construction and gravel pits. The elements most associated with PC1 (Al, Be, Ca, Fe, Mg, Rb, Y, and REEs) are typically found in silicate and carbonate minerals from dust, generally consistent with previous Wasatch Front dust studies (Goodman et al., 2019; Putman et al., 2022). The relative importance of dust to the Wasatch Front from local versus regional sources is not clear, with one recent study suggesting that the majority of dust at ground level is generated from local soil material (Putman et al., 2022) and others pointing to regional playas as the main dust source to rooftop samplers and mountain snowpack (Carling et al., 2020; Dastrup et al., 2018; Goodman et al., 2019). These apparent differences may be a result of sampling methods, with rooftop samplers and mountain snowpack more likely to receive far-travelled dust compared with ground level samplers in the urban area. The importance of regional playas, including Great Salt Lake, as dust sources to the Wasatch Mountains has been demonstrated using backward trajectory modeling (Lang et al., 2023; Skiles et al., 2018) and satellite imagery (Hahnenberger and Nicoll, 2012; Nicoll et al., 2020), yet it is also likely that local soil dust is important at ground level in the urban area. In our present study, we rely on time-series sampling of 87Sr/86Sr ratios to identify PM from local and regional sources (discussed in Section 4.2).

Urban pollution was identified as a source of trace elements in PM, particularly during winter months when the Wasatch Front experiences poor air quality during periods of persistent cold air pools. We use the term "urban pollution" generally because we are unable to determine the exact sources of As, Cd, Mo, Pb, Sb, Se, and Tl from our dataset. Urban pollution may include a variety of activities such as industry, vehicle exhaust and non-exhaust emissions, biomass burning, coal/oil combustion, and other sources (Hopke et al., 2020). The anthropogenic associated elements As, Cd, Pb, Sb, and Se were similarly elevated in Wasatch Front dust, and are discussed in greater detail, in prior studies (Goodman et al., 2019; Putman et al., 2022). Although not strictly urban pollution, mining and mineral processing are also trace metal sources along the Wasatch Front with the Kennecott copper mine and associated processing facilities (Fig. 1). Specifically, Cu, Mo, and Tl were mostly closely associated with mining pollution in the Wasatch Front in a previous study (Putman et al., 2022). Cu was grouped with fireworks in the PCA, but there is likely a substantial portion of Cu from mining pollution in our samples as noted by increased Cu concentrations during winter (Fig. 2).

The effect of fireworks smoke on atmospheric trace element concentrations has been observed in other locations. Smoke from fireworks is an important short-term source of anthropogenic pollutants that impacts local air quality (Singh et al., 2019), water quality (Wilkin et al., 2007), and snowpack (Steinhauser et al., 2008). The elements Ba, Cu, K, Mg, and Sr are typically used as tracers of fireworks PM to better understand the effect of fireworks on air quality (Singh et al., 2019; Vecchi et al., 2008). We observed increases in all of these elements except Mg, which may reflect a naturally high Mg background in the Wasatch Front because it is surrounded by Mg-rich carbonate rocks and playas (Goodman et al., 2019). Notably, Cr and V were also grouped with the fireworks elements in PC3. These are minor components of fireworks that nonetheless may be associated with fireworks smoke (Dutcher et al., 1999; Kosanke et al., 2013).

Other types of air quality impacts were not identified with our dataset, such as pollution from NAAQS priority pollutants  $O_3$ ,  $NO_2$ ,  $SO_2$ , and CO, or pollution from wildfire smoke, because we lacked measurements of specific compounds to recognize these pollution sources. Wildfire smoke commonly contributes to poor air quality along the Wasatch Front during summer and fall (Mallia et al., 2020). However, in

our study the effect of wildfires was indistinguishable from other signatures. The metals Cd, Cu, Pb, Sn, and Zn are enriched in wildfire smoke and burned soils (Jovanovic et al., 2011; Sparks and Wagner, 2021), but these metals did not show a clear trend that was distinguishable from summertime mineral dust. To better identify wildfire smoke, other tracers need to be included such as organic compounds along with trace element chemistry (Schneider and Abbatt, 2022).

Our study spanned COVID-19 lockdowns during 2020 that may have affected observed trace element concentrations. Numerous studies have documented the effects of COVID-19 lockdowns on air quality, including reduced levels of PM<sub>2.5</sub>, NO<sub>2</sub>, O<sub>3</sub>, and metal concentrations (Adam et al., 2021; Gautam, 2020; Jephcote et al., 2021; Ming et al., 2020; Yushin et al., 2020). We observed lower concentrations of specific trace elements during summer 2020 relative to 2021, possibly due to reduced air pollution during COVID-19 lockdowns. For example, As, Cd, and Pb concentrations were generally lower during summer 2020 (the height of the lockdowns) relative to summer 2021 (after most restrictions had lifted) (Fig. 3). However, concentrations of these elements were relatively higher during January 2021 (when some COVID-19 restrictions were still in place) relative to January 2020 (before COVID-19 lockdowns). The year-to-year differences may also be due to differences in weather events across the sampling periods.

### 4.2. Sources of Sr in Wasatch front particulate matter

The <sup>87</sup>Sr/<sup>86</sup>Sr ratios revealed that a variety of sources contributed Sr to PM in the Wasatch Front. Dust from regional playas likely contributed to observed <sup>87</sup>Sr/<sup>86</sup>Sr ratios on our PM filters in Provo. We identified ten dust events between May 2019 and September 2021 with measured <sup>87</sup>Sr/<sup>86</sup>Sr ratios on corresponding filters ranging from 0.7099 to 0.7125, which falls within the range of expected values for dust from Sevier Dry Lake (~0.7100), Great Salt Lake (~0.7150), and other regional playas (~0.7120) (Carling et al., 2020). Playa dust apparently plays a major role in <sup>87</sup>Sr/<sup>86</sup>Sr ratios of urban dust, as proposed in an earlier study (Carling et al., 2020). Dust from the dry lakebed of Great Salt Lake may become an increasing problem with declining lake levels and further damage to the soil crust.

Fugitive dust from local gravel pits and construction sites also likely contributed to observed <sup>87</sup>Sr/<sup>86</sup>Sr ratios on the PM filters. Samples downwind of an active gravel mine showed an 87Sr/86Sr value of  $\sim$ 0.7120 (Fig. 6). This value is consistent with previous measurements of <sup>87</sup>Sr/<sup>86</sup>Sr ratios in Lake Bonneville shoreline sediments (Blakowski et al., 2022; Hart et al., 2004), the primary formation targeted by sand and gravel mine operations along the Wasatch Front. Other local sources may contribute to observed <sup>87</sup>Sr/<sup>86</sup>Sr ratios in PM, such as fugitive dust from roads, construction, and mining (Putman et al., 2022). Particulate matter from sources not sampled would also affect measured <sup>87</sup>Sr/<sup>86</sup>Sr ratios. Local bedrock formations from the Carboniferous to Permian including the Great Blue Limestone and Deseret Limestone have <sup>87</sup>Sr/<sup>86</sup>Sr ratios ~0.7080 (Blumstein et al., 2004). Oligocene/Eocene volcanic fields of the eastern Great Basin have 87Sr/86Sr ratios from 0.7070 to 0.7080 (Wooden et al., 1999). Fugitive dust generated from these sources would create a mixture with lower <sup>87</sup>Sr/<sup>86</sup>Sr ratios relative to Sevier Dry Lake dust, which may explain why many of the  ${}^{87}\text{Sr}/{}^{86}\text{Sr}$ ratios are slightly below 0.710 at Provo (Fig. 6). Measurements of additional isotopic systems, such as Pb or Nd isotopes, would provide further insight to distinguish PM inputs from mineral dust and urban aerosols (Munroe, 2014; Widory et al., 2010).

In addition to playas and fugitive dust, fireworks smoke contributed to  $^{87}\text{Sr}/^{86}\text{Sr}$  ratios of urban dust. The lowest  $^{87}\text{Sr}/^{86}\text{Sr}$  ratios were recorded during July each year associated with the Independence Day holiday. The effect of fireworks was observed over the Independence Day holiday in 2009 in Salt Lake City and 2019, 2020, and 2021 in Provo with relatively low  $^{87}\text{Sr}/^{86}\text{Sr}$  ratios measured on corresponding filters. While we were unable to find published values of  $^{87}\text{Sr}/^{86}\text{Sr}$  ratios for fireworks, we assume that the value is at or below 0.7080 because

mixing of low <sup>87</sup>Sr/<sup>86</sup>Sr ratios from fireworks with ambient PM would generate observed ratios between 0.708 and 0.709 during fireworks events. Fireworks are an unexpected control on <sup>87</sup>Sr/<sup>86</sup>Sr ratios of PM that was only identifiable with a time-series dataset. Other studies relying on measurements that integrate several months of bulk deposition may overlook the impacts of fireworks. For example, the relatively low <sup>87</sup>Sr/<sup>86</sup>Sr ratios of urban dust in months-integrated samples (Putman et al., 2022) may be partially explained by deposition of smoke from fireworks.

### 4.3. Implications for public health

The environmentally available fraction of toxic elements may have implications for human and environmental health as these elements may be taken up by animals and plants. Our results indicate that in an urban setting, a majority of potentially toxic elements such as As, Cd, Cu, Mo, Pb, and Se, and U may be bioavailable through inhalation or uptake by plants. These elements are contributed to the atmosphere mostly through anthropogenic pollution and accumulate in the air during winter inversions. Fireworks also contributed readily available forms of Sr, K, Ba, and Cu to atmospheric PM. Elements found in evaporite and carbonate minerals, including Na, Ca, and Mg, were readily leached but likely do not contribute to health concerns. Currently, Pb is the only metal listed with a NAAQS standard and our samples were below health thresholds. However, it is not clear at what concentrations Pb or other metals may cause harm from acute or chronic effects. One limitation in using sequential leaching results to infer bioavailability is that these are operationally defined solubilities that may not reflect actual availability by plants and animals (Tessier and Campbell, 1987).

Our study represents point measurements from two locations within the urban area but spatial differences in trace metal concentrations are likely important. A spatial analysis of trace metal exposure across the northern Wasatch Front suggests that marginalized groups in neighborhoods along the industrial and commercial corridor may be at increased risk from trace metals in dust (Putman et al., 2022). Further work is needed to determine health impacts across communities in the southern Wasatch Front to determine potential impacts on lower income neighborhoods.

### 5. Conclusions

Atmospheric trace element concentrations measured on particulate matter filters collected along the Wasatch Front, Utah, suggest that mineral dust, urban pollution, and fireworks are the main sources contributing to poor air quality in a complex urban environment. Raw chemistry data and principal components analysis were useful for identifying sources affecting air quality. In particular, plotting principal component scores as a time-series revealed how the primary dust sources changed seasonally. Dust from regional playas in the Great Basin and local fugitive dust from gravel pits and other sources affect air quality during spring through fall. Winter inversions contribute to relatively high concentrations of toxic metals, including As, Cd, Pb and Tl during December through February. Fireworks also contribute significant amounts atmospheric metals over short time periods, contributing Ba, Cu, K, and Sr during holidays. Strontium isotope ( $^{87}\mathrm{Sr}/^{86}\mathrm{Sr}$ ) ratios were used to identify dust sources from regional playas, local gravel pits, and fireworks events over multiple years. The <sup>87</sup>Sr/<sup>86</sup>Sr ratios of particulate matter were especially low during the Independence Day holiday, showing the utility of <sup>87</sup>Sr/<sup>86</sup>Sr ratios as a tracer of fireworks smoke. We found that specific trace elements, including As, Cd, Cu, Mo, Pb, Se, and U, were environmentally available and may have a negative impact on human health. Through an analysis of geochemical fingerprints of urban particulate matter, our study has implications for understanding sources of atmospheric trace elements that contribute to poor air quality. High frequency particulate matter sampling combined with geochemical and isotopic measurements may prove useful for pollution source monitoring in urban areas worldwide.

### CRediT authorship contribution statement

Micah J. Marcy: Data curation, Formal analysis, Investigation, Methodology, Writing – original draft. Gregory T. Carling: Conceptualization, Data curation, Formal analysis, Funding acquisition, Investigation, Methodology, Project administration, Resources, Software, Supervision, Validation, Visualization, Writing – original draft, Writing – review & editing. Alyssa N. Thompson: Investigation, Methodology, Writing – original draft. Barry R. Bickmore: Data curation, Formal analysis, Supervision, Validation, Visualization, Writing – original draft, Writing – review & editing. Stephen T. Nelson: Formal analysis, Supervision, Writing – original draft. Kevin A. Rey: Investigation, Methodology, Supervision, Writing – original draft. Diego P. Fernandez: Investigation, Methodology, Supervision, Writing – original draft. Matthew Heiner: Data curation, Formal analysis, Visualization, Writing – original draft. Bradley R. Adams: Conceptualization, Funding acquisition, Project administration, Writing – original draft.

### **Declaration of competing interest**

The authors declare that they have no known competing financial interests or personal relationships that could have appeared to influence the work reported in this paper.

### Data availability

All data used in this study are available in the EarthChem repository at https://doi.org/10.26022/IEDA/112910

# Acknowledgments

This work was supported by a Science for Solutions grant from the Utah Division of Air Quality and by the U.S. National Science Foundation grant EAR-2012093. Any opinions, findings and conclusions or recommendations expressed are those of the authors and do not necessarily reflect the views of the Division of Air Quality or the National Science Foundation.

# Appendix A. Supplementary data

Supplementary data to this article can be found online at https://doi.org/10.1016/j.apgeochem.2024.105906.

# References

- Aarons, S.M., Blakowski, M.A., Aciego, S.M., Stevenson, E.I., Sims, K.W.W., Scott, S.R., Aarons, C., 2017. Geochemical characterization of critical dust source regions in the American West. Geochem. Cosmochim. Acta 215, 141–161.
- Abuduwaili, J., Gabchenko, M.V., Junrong, X., 2008. Eolian transport of salts—a case study in the area of Lake Ebinur (Xinjiang, Northwest China). J. Arid Environ. 72, 1843–1852.
- Adam, M.G., Tran, P.T.M., Balasubramanian, R., 2021. Air quality changes in cities during the COVID-19 lockdown: a critical review. Atmos. Res. 264, 105823.
- Blakowski, M.A., Putman, A.L., Jones, D.K., DiViesti, D.N., Hynek, S.A., Fernandez, D.P., Mendoza, D., 2022. Dust and Sediment Data from Great Salt Lake and the Wasatch Front, Utah, 2018-19. U.S. Geological Survey data release.
- Blumstein, A.M., Elmore, R.D., Engel, M.H., Elliot, C., Basu, A., 2004. Paleomagnetic dating of burial diagenesis in Mississippian carbonates, Utah. J. Geophys. Res. Solid Earth 109 n/a-n/a.
- Carling, G.T., Fernandez, D.P., Johnson, W.P., 2012. Dust-mediated loading of trace and major elements to Wasatch Mountain snowpack. Sci. Total Environ. 432, 65–77.
- Carling, G.T., Fernandez, D.P., Rey, K.A., Hale, C.A., Goodman, M.M., Nelson, S.T., 2020. Using strontium isotopes to trace dust from a drying Great Salt Lake to adjacent urban areas and mountain snowpack. Environ. Res. Lett. 15, 114035.
- Dastrup, D.B., Carling, G.T., Collins, S.A., Nelson, S.T., Fernandez, D.P., Tingey, D.G., Hahnenberger, M., Aanderud, Z.T., 2018. Aeolian dust chemistry and bacterial communities in snow are unique to airshed locations across northern Utah, USA. Atmos. Environ. 193, 251–261.

- Dutcher, D.D., Perry, K.D., Cahill, T.A., Copeland, S.A., 1999. Effects of indoor pyrotechnic displays on the air quality in the Houston astrodome. J. Air Waste Manag. Assoc. 49, 156–160.
- Gautam, S., 2020. The influence of COVID-19 on air quality in India: a boon or inutile. Bull. Environ. Contam. Toxicol. 104, 724–726.
- Gillies, R.R., Wang, S.-Y., Booth, M.R., 2010. Atmospheric scale interaction on wintertime intermountain west low-level inversions. Weather Forecast. 25, 1196–1210.
- Goodman, M.M., Carling, G.T., Fernandez, D.P., Rey, K.A., Hale, C.A., Bickmore, B.R., Nelson, S.T., Munroe, J.S., 2019. Trace element chemistry of atmospheric deposition along the Wasatch Front (Utah, USA) reflects regional playa dust and local urban aerosols. Chem. Geol. 530, 119317.
- Goudie, A.S., 2009. Dust storms: recent developments. J. Environ. Manag. 90, 89–94.
   Hahnenberger, M., Nicoll, K., 2012. Meteorological characteristics of dust storm events in the eastern Great Basin of Utah. U.S.A. Atmospheric Environment 60, 601–612.
- Hart, W.S., Quade, J., Madsen, D.B., Kaufman, D.S., Oviatt, C.G., 2004. The 87Sr/86Sr ratios of lacustrine carbonates and lake-level history of the Bonneville paleolake system. Geol. Soc. Am. Bull. 116, 1107.
- Hopke, P.K., Dai, Q., Li, L., Feng, Y., 2020. Global review of recent source apportionments for airborne particulate matter. Sci. Total Environ. 740, 140091.
- Jephcote, C., Hansell, A.L., Adams, K., Gulliver, J., 2021. Changes in air quality during COVID-19 'lockdown' in the United Kingdom. Environ. Pollut. 272, 116011.
- Jovanovic, V.P.S., Ilic, M.D., Markovic, M.S., Mitic, V.D., Nikolic Mandic, S.D., Stojanovic, G.S., 2011. Wild fire impact on copper, zinc, lead and cadmium distribution in soil and relation with abundance in selected plants of Lamiaceae family from Vidlic Mountain (Serbia). Chemosphere 84, 1584–1591.
- Kosanke, K., Kosanke, B., Sturman, B., Shimizu, T., Wilson, M.A., Maltitz, I.v., Kubota, N., Jennings-White, C., Chapman, D., Dillehay, D.R., Smith, T., Podlesak, M., 2013. Pyrotechnic Chemistry. Pyrotechnic Reference Series No, 4. Journal of Pyrotechnics, Whitewater, CO, pp. 416–pp.
- Kulkarni, P., Chellam, S., Fraser, M.P., 2007. Tracking petroleum refinery emission events using lanthanum and lanthanides as elemental markers for PM2.5. Environ. Sci. Technol. 41, 6748–6754.
- Lang, O.I., Mallia, D., McKenzie Skiles, S., 2023. The shrinking Great Salt Lake contributes to record high dust-on-snow deposition in the Wasatch Mountains during the 2022 snowmelt season. Environ. Res. Lett. 18, 064045.
- Lanno, R., Wells, J., Conder, J., Bradham, K., Basta, N., 2004. The bioavailability of chemicals in soil for earthworms. Ecotoxicol. Environ. Saf. 57, 39–47.
- Mackey, G.N., Fernandez, D.P., 2011. High Throughput Sr Isotope Analysis Using an Automated Column Chemistry System. AGU Fall Meeting.
- Mallia, D.V., Kochanski, A.K., Kelly, K.E., Whitaker, R., Xing, W., Mitchell, L.E., Jacques, A., Farguell, A., Mandel, J., Gaillardon, P.E., 2020. Evaluating wildfire smoke transport within a coupled fire-atmosphere model using a high-density observation network for an episodic smoke event along Utah's Wasatch Front. J. Geophys. Res. Atmos. 125, e2020JD032712.
- Miller-Schulze, J.P., Shafer, M., Schauer, J.J., Heo, J., Solomon, P.A., Lantz, J., Artamonova, M., Chen, B., Imashev, S., Sverdlik, L., Carmichael, G., DeMinter, J., 2015. Seasonal contribution of mineral dust and other major components to particulate matter at two remote sites in Central Asia. Atmos. Environ. 119, 11–20.
- Ming, W., Zhou, Z., Ai, H., Bi, H., Zhong, Y., 2020. COVID-19 and air quality: evidence from China. Emerg. Mark. Finance Trade 56, 2422–2442.
- Moreno, T., Karanasiou, A., Amato, F., Lucarelli, F., Nava, S., Calzolai, G., Chiari, M., Coz, E., Artínano, B., Lumbreras, J., Borge, R., Boldo, E., Linares, C., Alastuey, A., Querol, X., Gibbons, W., 2013. Daily and hourly sourcing of metallic and mineral dust in urban air contaminated by traffic and coal-burning emissions. Atmos. Environ. 68, 33–44.
- Munroe, J.S., 2014. Properties of modern dust accumulating in the Uinta Mountains, Utah, USA, and implications for the regional dust system of the Rocky Mountains. Earth Surf. Process. Landforms 39, 1979–1988.
- Munroe, J.S., Norris, E.D., Carling, G.T., Beard, B.L., Satkoski, A.M., Liu, L., 2019. Isotope fingerprinting reveals western North American sources of modern dust in the Uinta Mountains, Utah, USA. Aeolian Research 38, 39–47.
- Naiman, Z., Quade, J., Patchett, P.J., 2000. Isotopic evidnence for eolian recycling of pedogenic carbonate and variations in carbonate dust sources throughout the southwest United States. Geochem. Cosmochim. Acta 64, 3099–3109.
- Nicoll, K., Hahnenberger, M., Goldstein, H.L., 2020. 'Dust in the wind' from source-tosink: analysis of the 14–15 April 2015 storm in Utah. Aeolian Research 46, 100532.

- Oviatt, C.G., 1988. Late Pleistocene and holocene lake fluctuations in the sevier lake basin, Utah, USA. J. Paleolimnol. 1, 9–21.
- Perry, K.D., 1999. Effects of outdoor pyrotechnic displays on the regional air quality of western Washington state. J. Air Waste Manag. Assoc. 49, 146–155.
- Pope, A.C., Dockery, D.W., Spengler, J.D., Raizenne, M.E., 1990. Respiratory Health and PM10 Pollution: A Daily Time Series Analysis. American Review of Respiratory Diseases.
- Putman, A.L., Jones, D.K., Blakowski, M.A., DiViesti, D., Hynek, S.A., Fernandez, D.P., Mendoza, D., 2022. Industrial particulate pollution and historical land use contribute metals of concern to dust deposited in neighborhoods along the Wasatch front. UT, USA GeoHealth 6, e2022GH000671.
- Reheis, M.C., Kihl, R., 1995. Dust deposition in southern Nevada and California, 1984–1989: relations to climate, source area, and source lithology. J. Geophys. Res. 100, 8893.
- Reynolds, R.L., Goldstein, H.L., Moskowitz, B.M., Bryant, A.C., Skiles, S.M., Kokaly, R.F., Flagg, C.B., Yauk, K., Berquó, T., Breit, G., Ketterer, M., Fernandez, D., Miller, M.E., Painter, T.H., 2014. Composition of dust deposited to snow cover in the Wasatch Range (Utah, USA): controls on radiative properties of snow cover and comparison to some dust-source sediments. Aeolian Research 15, 73–90.
- Reynolds, R.L., Mordecai, J.S., Rosenbaum, J.G., Ketterer, M.E., Walsh, M.K., Moser, K. A., 2010. Compositional changes in sediments of subalpine lakes, Uinta Mountains (Utah): evidence for the effects of human activity on atmospheric dust inputs. J. Paleolimnol. 44, 161–175.
- Schneider, S.R., Abbatt, J.P.D., 2022. Wildfire atmospheric chemistry: climate and air quality impacts. Trends in Chemistry 4, 255–257.
- Singh, A., Pant, P., Pope, F.D., 2019. Air quality during and after festivals: aerosol concentrations, composition and health effects. Atmos. Res. 227, 220–232.
- Skiles, S.M., Derek, V.M., Hallar, A.G., John, C.L., Andrew, L., Ross, P., Steven, C., 2018. Implications of a shrinking Great Salt Lake for dust on snow deposition in the Wasatch Mountains, UT, as informed by a source to sink case study from the 13–14 April 2017 dust event. Environ. Res. Lett. 13, 124031.
- Sparks, T.L., Wagner, J., 2021. Composition of particulate matter during a wildfire smoke episode in an urban area. Aerosol. Sci. Technol. 55, 734–747.
- Steenburgh, W., Massey, J.D., Painter, T.H., 2012. Episodic dust events of Utah's Wasatch front and adjoining region. J. Appl. Meteorol. Climatol. 51, 1654–1669.
- Steiger, R.H., Jäger, E., 1977. Subcommission on geochronology: convention on the use of decay constants in geo- and cosmochronology. Earth Planet Sci. Lett. 36, 359–362.
- Steinhauser, G., Sterba, J.H., Foster, M., Grass, F., Bichler, M., 2008. Heavy metals from pyrotechnics in new years Eve snow. Atmos. Environ. 42, 8616–8622.
- Sudheer, A.K., Rengarajan, R., 2012. Atmospheric mineral dust and trace metals over urban environment in western India during winter. Aerosol Air Qual. Res. 12, 923–933.
- Sun, J., Shen, Z., Zhang, L., Lei, Y., Gong, X., Zhang, Q., Zhang, T., Xu, H., Cui, S., Wang, Q., Cao, J., Tao, J., Zhang, N., Zhang, R., 2019. Chemical source profiles of urban fugitive dust PM2.5 samples from 21 cities across China. Sci. Total Environ. 649, 1045–1053.
- Tessier, A., Campbell, P.G.C., 1987. Partitioning of trace metals in sediments: relationships with bioavailability. Hydrobiologia 149, 43–52.
- USGS, 2023. Great Salt Lake Hydro Mapper.
- Vecchi, R., Bernardoni, V., Cricchio, D., D'Alessandro, A., Fermo, P., Lucarelli, F., Nava, S., Piazzalunga, A., Valli, G., 2008. The impact of fireworks on airborne particles. Atmos. Environ. 42, 1121–1132.
- Whiteman, C.D., Hoch, S.W., Horel, J.D., Charland, A., 2014. Relationship between particulate air pollution and meteorological variables in Utah's Salt Lake Valley. Atmos. Environ. 94, 742–753.
- Widory, D., Liu, X., Dong, S., 2010. Isotopes as tracers of sources of lead and strontium in aerosols (TSP & PM2.5) in Beijing. Atmos. Environ. 44, 3679–3687.
- Wilkin, R.T., Fine, D.D., Burnett, N.G., 2007. Perchlorate behavior in a municipal lake following fireworks displays. Environ. Sci. Technol. 41, 3966–3971.
- Wolyn, P.G., McKee, T.B., 1989. Deep stable layers in the intermountain western United States. Mon. Weather Rev. 117, 461–472.
- Wooden, J.L., Kistler, R.W., Tosdal, R.M., 1999. Strontium, lead, and oxygen isotopic data for granitoid and volcanic rocks from the northern Great Basin and Sierra Nevada, California, Nevada and Utah. In: Open-File Report, - ed.
- Yushin, N., Chaligava, O., Zinicovscaia, I., Vergel, K., Grozdov, D., 2020. Mosses as bioindicators of heavy metal air pollution in the lockdown period adopted to cope with the COVID-19 pandemic. Atmosphere 11, 1194.